

## Preparation of Nickel Sulfide Thin Films by Electroreduction of Aqueous $\text{Ni}^{2+}$ - $\text{SCN}^-$ Complex

Koichi Yamaguchi, Tsukasa Yoshida, Dinesh P. Amalnerkar and Hideki Minoura

Environmental and Renewable Energy System (ERES) Division, Graduate School of Engineering,  
Gifu University, Yanagido 1-1, Gifu 501-1193, Japan  
Fax: +81-58-293-2587, e-mail: yama@apchem.gifu-u.ac.jp

Electrochemical reduction of  $\text{Ni}^{2+}$ - $\text{SCN}^-$  complex in aqueous solutions has been examined for the deposition of nickel sulfide thin films. Formation of  $\text{Ni}_3\text{S}_2$ , amorphous, metallic Ni phases were found by XRD analysis. The chemical composition of the film is under control of the deposition potential as well as the composition of the plating bath. When thickness of the films deposited at various potentials but for a fixed passed charge are compared, the film thickness tends to increase upon positive shift of the potentials, along with a decrease in atomic percent of Ni in the deposited film. The same trend is found when the  $\text{SCN}^-$  content in the bath is increased at a fixed deposition potential. This change of the film thickness has been reasonably explained by the change of the average density of the deposited films which are mixtures of NiS,  $\text{Ni}_3\text{S}_2$  and Ni.

Keywords : nickel sulfide, thin film, electrodeposition, thiocyanate

### 1. INTRODUCTION

Techniques for the preparation of thin films of inorganic compound from aqueous solutions have received an immense attention in recent years, because of inherent advantages related to cost-effective and environmentally benign film processing, as compared to the gas-phase techniques which inevitably demand high temperature and/or vacuum. [1] Although the solution phase techniques were thought to yield poor quality films compared to the gas-phase techniques, we have recently realized an ordered growth of CdS thin films by electroreduction of  $\text{Cd}^{2+}$ - $\text{SCN}^-$  aqueous complex [2]. In a quest to extend the utility of such techniques in developing thin films of other important inorganic compounds, we have recently explored the possibility of producing nickel sulfide thin films having widespread applications from ferromagnetic materials [3] to catalysis [4,5]. The chemical stability of  $\text{Ni}^{2+}$ - $\text{SCN}^-$  complex and its electrochemical reactivity to yield NiS [6,7] were also important considerations in exploring the present work. The preliminary account of such exploratory research is furnished in this paper.

### 2. EXPERIMENTAL

#### 2.1 Materials

Nickel chloride ( $\text{NiCl}_2$ ) and potassium thiocyanate (KSCN) were purchased from Kishida Chemical Co. Ltd. and used as received. Aqueous mixture of  $\text{NiCl}_2$  and KSCN served as plating baths. Before each experiment, Ar gas was purged in the plating bath for 15 min. The pH of the plating bath was confirmed to be around 6. An indium tin oxide (ITO) coated glass ( $10\Omega/\text{sq}$ , purchased from Musashino Fine Glass Co. Ltd.) was used as a substrate. In order to obtain hydrophilic surface on a substrate, it was cleaned by sequentially dipping into an aqueous solution containing 0.5wt% detergent (Vista, AIC Co. Ltd.) and in acetone each for 10 min and in 1 M  $\text{HNO}_3$  ( $M = \text{mol}/\text{dm}^3$ ) for 1 min, followed by rinsing

with water. Doubly distilled and ion exchanged water was used throughout all the experiments.

#### 2.2 Experimental setup for the film deposition

The film deposition was carried out potentiostatically in a single compartment three-electrode system comprising of an ITO substrate, a platinized Pt plate and a saturated calomel electrode (SCE) as working, counter and reference electrodes, respectively. The temperature of the plating bath was kept at 70 °C by a thermostat bath. The electrochemical measurements and the potentiostatic electrolysis were performed on a potentiostat equipped with a function generator (Nikko Keisoku NPGFZ-2501-A). The cyclic voltammograms were recorded by an X-Y recorder (Graphtec WX-1200). Passed charge during the electrodeposition was monitored by a digital coulomb meter (Nikko Keisoku NDCM-4).

#### 2.3 Physico-chemical characterization of films

The crystallographic structure of the deposited films was examined by an X-ray diffractometer with  $\text{Cu K}\alpha$  radiation (Rigaku RAD-2R). The surface morphologies of films were observed by a scanning electron microscope (SEM, Topcon ABT-150FS) and by using an atomic force microscope (AFM, Seiko Instruments Inc. SPI3800N). The chemical composition of the films was determined by an energy dispersive X-ray analyzer (EDX, Horiba EMAX-2770). The film thickness was determined by a surface profilometer (Kosaka Lab. SE-2300).

### 3. RESULTS AND DISCUSSION

#### 3.1 Cyclic voltammetry

The electrochemical reactions in aqueous solutions containing  $\text{NiCl}_2$ , KSCN, or both of them have been studied by means of cyclic voltammetry. The resultant voltammograms are presented in Fig. 1. The cyclic voltammogram measured in a  $\text{NiCl}_2$  solution (curve a) shows an abrupt increase in a cathodic current from

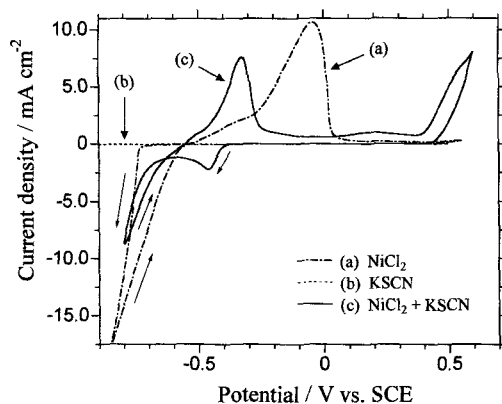
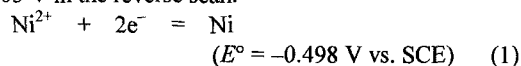
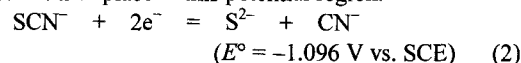


Fig. 1 Cyclic voltammograms measured at an ITO electrode in aqueous solutions containing (a) 0.05 M  $\text{NiCl}_2$  + 0.5 M  $\text{KCl}$ , (b) 0.5 M  $\text{KSCN}$  and (c) 0.05 M  $\text{NiCl}_2$  + 0.5 M  $\text{KSCN}$ . The measurements were performed under Ar atmosphere, at 70 °C and at a scan rate of 50  $\text{mVs}^{-1}$ .

around  $-0.75$  V in the negatively running scan due to the deposition of metallic Ni in accordance with eq. 1 and an anodic dissolution peak of deposited Ni at around  $-0.05$  V in the reverse scan.



In a  $\text{KSCN}$  solution (curve b), while the small cathodic current arises due to the reduction of proton [2], no other appreciable increase in the cathodic current is observed. The reduction of  $\text{SCN}^-$  ion to  $\text{S}^{2-}$  as expressed by eq. 2 does not take place in this potential region.



In the mixture of  $\text{NiCl}_2$  and  $\text{KSCN}$  (curve c), voltammograms were drastically changed compared to that in the solution containing only  $\text{NiCl}_2$  (curve a). It is important to note that a cathodic current flow is seen at around  $-0.40$  V for negatively running scan, which is not observed in curve a. It is obvious that an electrochemical reaction other than the deposition of metallic Ni takes place. Deposition of thin films of nickel sulfide was confirmed by potentiostatic electrolyses in the potential region where this particular cathodic current is observed. It was also noticed that the cathodic current during the film deposition was larger by one to two orders of magnitude and the rate of film growth was faster in the  $\text{Ni}^{2+}$ - $\text{SCN}^-$  system than those previously found in the  $\text{Cd}^{2+}$ - $\text{SCN}^-$  system [2]. The deposited films were homogeneous, well adherent to the substrate.

### 3.2 XRD analysis of the deposited films

Fig. 2 shows X-ray diffractograms of the films deposited at  $-0.5$ ,  $-0.6$ ,  $-0.7$ ,  $-0.8$  and  $-0.9$  V vs. SCE for a passed charge of 1.0  $\text{C/cm}^2$ . For the films deposited at  $-0.5$  and  $-0.6$  V, diffraction peaks assigned to  $\text{Ni}_3\text{S}_2$  phase are seen aside from those arising from the ITO substrate. It is worthwhile to note that earlier Krogulec et al. have studied the electrochemical reduction of  $\text{SCN}^-$  in the presence of  $\text{Ni}^{2+}$  at a dropping mercury electrode and they reported that electroreduction in the  $\text{Ni}^{2+}$ - $\text{SCN}^-$  system yields either metallic Ni or NiS via partially reduced state such as  $\text{Ni(I)-SCN}^-$  [6,7]. However, they have not mentioned about the formation of  $\text{Ni}_3\text{S}_2$  phase in their study. Besides, diffraction peaks attributable to various phases of nickel sulfide, such as

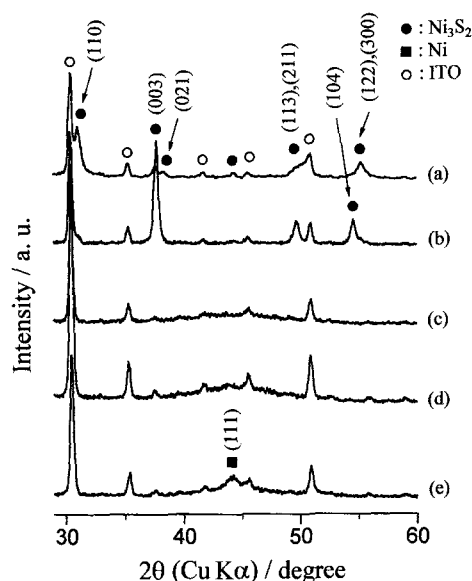


Fig. 2 X-ray diffractograms of the films electrodeposited on an ITO-coated glass in a 0.05 M  $\text{NiCl}_2$  + 0.5 M  $\text{KSCN}$  aqueous solution for a passed charge of 1.0  $\text{C/cm}^2$ . The deposition was carried out at (a)  $-0.5$ , (b)  $-0.6$ , (c)  $-0.7$ , (d)  $-0.8$  and (e)  $-0.9$  V vs. SCE and at 70 °C.

$\text{NiS}$ ,  $\text{Ni}_3\text{S}_4$ ,  $\text{Ni}_7\text{S}_6$ , are not found in the diffraction patterns of these films. When the deposition potential goes to more negative side, i.e.  $-0.7$  and  $-0.8$  V, there are no diffraction peaks other than those of the ITO, clearly indicating X-ray amorphous character of these films. For the deposits obtained at further negative potentials, i.e.  $-0.9$  V, a broad diffraction peak ascribable to metallic Ni (111) is seen, suggesting the formation of crystalline Ni. The gradual change in the crystal structure from  $\text{Ni}_3\text{S}_2$  to metallic Ni with the deposition potential toward the negative direction implies changes in the crystal phase as well as chemical composition of the deposited films.

### 3.3 Surface morphology of films

Surface morphologies of the deposited films have been studied by means of SEM and AFM. Fig. 3(a) shows an SEM image of a nickel sulfide film deposited at  $-0.6$  V for a passed charge of 1.0  $\text{C/cm}^2$ . The deposited films appear to be uniform and homogeneous with particles of around 500 nm in diameter. An AFM image of this film for the scanning area of  $1 \mu\text{m} \times 1 \mu\text{m}$  is reproduced in Fig. 3(b). It is clearly noticed from this image that each particle observed in Fig. 3(a) is composed of smaller particles of 30–50 nm in diameter. Considering the fact that the thickness of the film shown in Fig. 3 is ca. 700 nm, it could be concluded that the layer-by-layer growth mechanism suggested previously in the  $\text{Cd}^{2+}$ - $\text{SCN}^-$  system [2] may not be operative in the present case.

### 3.4 Effect of the deposition conditions on the chemical composition and thickness of films

As revealed by the XRD analysis, the chemical composition of the films is varied with the deposition conditions. We have further examined the chemical composition of the films by EDX. Fig. 4 shows the relationship between the atomic percent of Ni in the film (hereafter denoted as Ni(at%)) and the deposition potential, together with the thickness of corresponding films. Along with the negative shift of the deposition

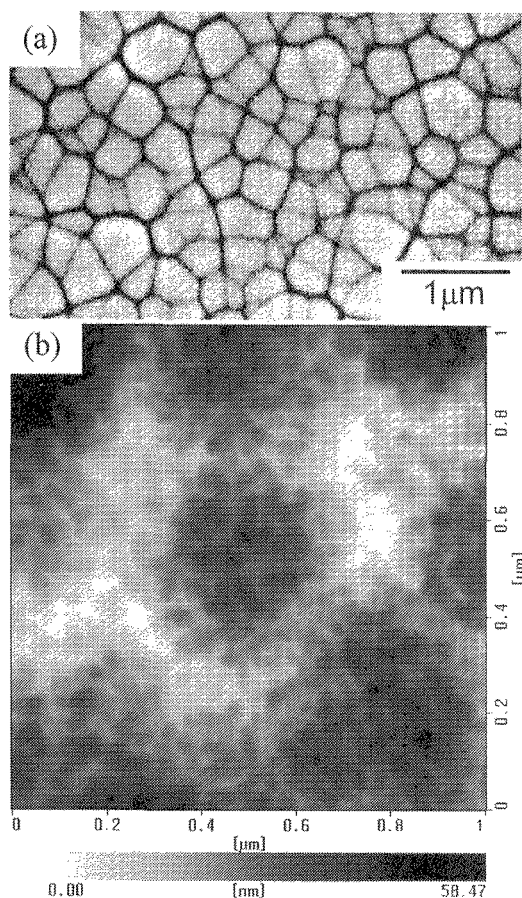


Fig. 3 (a) An SEM image of a nickel sulfide film electrodeposited in an aqueous mixture of 0.05 M NiCl<sub>2</sub> + 0.5 M KSCN at 70 °C for a passed charge of 1.0 C cm<sup>-2</sup>, (b) The AFM image of the same film. The gradation bar below the image indicates the difference in height from the lowest point to the highest one.

potential, Ni(at%) tends to increase with concomitant decrease of the film thickness. The same values were checked for the films deposited from baths containing variable amounts of KSCN, while a constant potential of -0.6 V vs. SCE is used (Fig. 5). As the concentration of KSCN decreases, Ni(at%) increases. The increase of Ni(at%) is accompanied with the decrease in the film thickness also in this case. These results evince that the chemical composition of the film can be controlled either by the deposition potential or by the composition of the plating bath.

The change of the film thickness with Ni(at%) can be reasonably explained by the change of the density of the films. The densities of metallic Ni, Ni<sub>3</sub>S<sub>2</sub> and NiS, as found from literature, are 8.91, 5.87 and 5.37, respectively. If the deposition of film is under the control of electrochemical reaction, a film with higher Ni(at%), which is deposited at a fixed passed charge, is expected to have lower density, resulting in thinner film thickness. Thus, theoretical calculation has been made in order to compare the thickness of the experimental values to that obtained by the calculation. Since crystalline phases of metallic Ni and Ni<sub>3</sub>S<sub>2</sub> have been found in the XRD pattern, it is reasonable to assume that the films down to Ni(at%) = 60% are mixtures of metallic Ni and Ni<sub>3</sub>S<sub>2</sub>. The overall composition of the films can therefore be

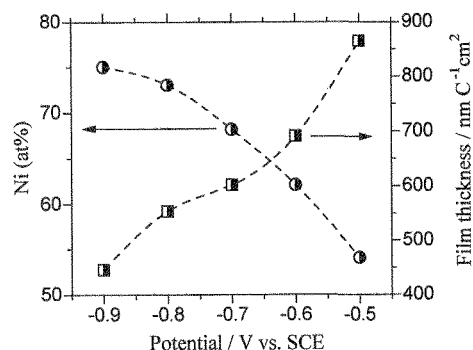


Fig. 4 Change of Ni(at%) and film thickness of deposits with deposition potential. The films were electrodeposited in a 0.05 M NiCl<sub>2</sub> + 0.5M KSCN aqueous solution for a passed charge of 1.0 C cm<sup>-2</sup> and at 70 °C.

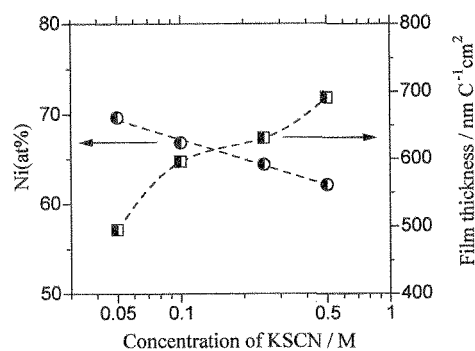


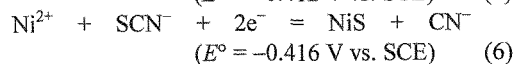
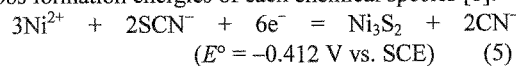
Fig. 5 Change of Ni(at%) and film thickness of deposits with KSCN concentration in the plating bath. The concentration of NiCl<sub>2</sub> was 0.05 M. The deposition was carried out at -0.6 V vs. SCE for a passed charge of 1.0 C cm<sup>-2</sup> and at 70 °C.

expressed as (Ni<sub>3</sub>S<sub>2</sub>)<sub>a</sub>Ni<sub>1-a</sub>. The film deposited at -0.5 V, in which Ni(at%) is less than 60 %, may comprise from mixture of Ni<sub>3</sub>S<sub>2</sub> and NiS for which Ni(at%) = 50 %. The overall composition of the film, in this case, is (Ni<sub>3</sub>S<sub>2</sub>)<sub>b</sub>(NiS)<sub>1-b</sub>. When *x* is atomic ratio of Ni in the film, the proportion parameters *a* and *b* are related to *x*, as

$$a = (2 - 2x)/(3x - 1) \quad (3)$$

$$b = (2x - 1)/(2 - 3x) \quad (4)$$

The electrochemical formation of Ni<sub>3</sub>S<sub>2</sub> and NiS can be described by eqs. 3 and 4, respectively. The standard potentials of these equations were calculated by using Gibbs formation energies of each chemical species [8].



If we assume that the films are dense and the faradaic efficiencies for the reactions of eqs. 1, 5, 6 are unity, the film thickness of Ni, Ni<sub>3</sub>S<sub>2</sub>, NiS and mixture of these can be estimated from the passed charge. From the faraday laws in eqs. 1, 5, 6, and using formulae weight, *M<sub>ij</sub>* [g mol<sup>-1</sup>], and density, *d<sub>ij</sub>* [g cm<sup>-3</sup>], of Ni<sub>3</sub>S<sub>2</sub>, the film thickness *t* [μm] can be related to the passed charge, *q* [C cm<sup>-2</sup>], by eqs. 7 (0.6 ≤ *x* ≤ 1.0) and 8 (0.5 ≤ *x* ≤ 0.6).

$$t = 10^4 \left( \frac{qM_{32}}{6Fd_{32}} a + \frac{qM_{10}}{2Fd_{10}} (1-a) \right) \quad (7)$$

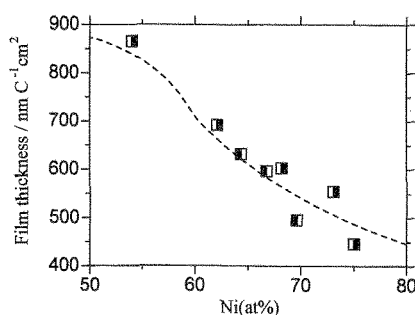


Fig. 6 Relationship between film thickness and Ni(at%). Hashed line shows the calculated values from eqs 7' and 8'. Square symbols show the experimental values taken from Figs. 4 and 5.

$$t = 10^4 \left( \frac{qM_{32}}{6Fd_{32}}b + \frac{qM_{11}}{2Fd_{11}}(1-b) \right) \quad (8)$$

where  $F$  is faradaic constant ( $= 9.65 \times 10^4 \text{ C mol}^{-1}$ ). Solving the two equations for  $x$  using the relationships of eqs. 3 and 4 yields

$$t = \frac{10^4 q}{F} \left( \left( \frac{M_{32}}{6d_{32}} - \frac{M_{10}}{2d_{10}} \right) \left( \frac{2-2x}{3x-1} \right) + \frac{M_{10}}{2d_{10}} \right) \quad (7')$$

$$t = \frac{10^4 q}{F} \left( \left( \frac{M_{32}}{6d_{32}} - \frac{M_{11}}{2d_{11}} \right) \left( \frac{2x-1}{2-3x} \right) + \frac{M_{11}}{2d_{11}} \right) \quad (8')$$

The relationship between the film thickness and Ni(at%) as predicted from eqs. 7' and 8' for  $q = 1 \text{ C cm}^{-2}$  is shown by a hashed line in Fig. 6. In the figure are also plotted the experimental values taken from Figs. 4 and 5. The experimental values quite nicely fit with the calculated curve, validating the assumptions taken in the discussion mentioned above.

The Ni(at%) in the films became higher when the films were deposited at more negative potential (Fig. 4) and when the KSCN concentration in the plating bath was lower (Fig. 5). Since the standard potentials for the deposition of both NiS and Ni<sub>3</sub>S<sub>2</sub> given in eqs. 3 and 4 are similar to that for the deposition of metallic Ni (eq. 1), formation of both nickel sulfide and metallic Ni is thermodynamically possible at the deposition potentials used in this study. Krogulec et al. observed that the efficiency of NiS formation in the Ni<sup>2+</sup>-SCN<sup>-</sup> system decreases at negative potentials [6]. They explained that the rate constant for the formation of NiS is constant while that for the deposition of Ni increases at negative potentials. The change of Ni(at%) in the films with deposition potential shown in Fig. 4 is consistent with the tendency reported by Krogulec et al. [6]. Fig. 7 depicts the change of Ni<sup>2+</sup> species in the plating bath as a function of the concentration of KSCN, where the total concentration of Ni<sup>2+</sup> species is set to 0.05 M. The formation constants ( $\log K_n$ ) for nickel thiocyanato complexes, [Ni(SCN)]<sup>+</sup>, Ni(SCN)<sub>2</sub>, [Ni(SCN)<sub>3</sub>]<sup>-</sup> are 1.18, 1.64 and 1.81, respectively [9], which are used in determining the concentrations of the stated Ni species. It is seen from Fig. 7 that about 70 % of Ni<sup>2+</sup> species exists as free Ni<sup>2+</sup> ion at the KSCN concentration of 0.05 M. As the KSCN concentration increases, the concentration of free Ni<sup>2+</sup> gradually decreases. Although the deposition of metallic Ni is possible from both thiocyanate complexes of Ni<sup>2+</sup> and free Ni<sup>2+</sup> ion, the further reduction of the intermediate Ni(I)-SCN<sup>-</sup> species

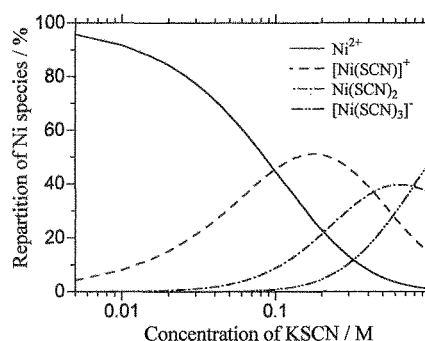


Fig. 7 Distribution of Ni<sup>2+</sup> species in the aqueous Ni<sup>2+</sup>-SCN<sup>-</sup> system as a function of the concentration of KSCN, calculated at pH 6 and at the total Ni<sup>2+</sup> concentration of 0.05 M.

to metallic Ni is relatively slow compared to the NiS formation [6]. The observed increase in Ni(at%) with decrease of the concentration of KSCN in the plating bath is attributable to the relative increase on the deposition rate of metallic Ni compared to the that of nickel sulfide due to the increase of the free Ni<sup>2+</sup> concentration.

In summary, formation of nickel sulfide thin films has been realized by electroreduction of aqueous Ni<sup>2+</sup>-SCN<sup>-</sup> complex. The chemical composition of the film can be controlled by the deposition potential as well as the composition of the plating bath. The mechanisms for the deposition of nickel sulfide thin films as well as the formation of crystalline Ni<sub>3</sub>S<sub>2</sub> phase in this system is still perplexing and yet to be clarified through future investigations.

#### Acknowledgment

The present work is partly defrayed by the Grant-in-Aid for Scientific Research on Priority-Area-Research "Electrochemistry of Ordered Interfaces" from the Ministry of Education, Science, Sports and Culture of Japan (09237105). K. Y. is grateful to JSPS Research Fellowships for Young Scientists. D. P. A. gratefully acknowledges the generous financial support extended by AIEJ for his stay at Gifu University.

#### References

- [1] M. Yoshimura, W. L. Suchanek and K. Byrappa, *MRS Bull.*, **25**, 17 (2000).
- [2] T. Yoshida, K. Yamaguchi, T. Kazitani, T. Sugiura and H. Minoura, *J. Electroanal. Chem.*, **473**, 209 (1999).
- [3] N. Sulitanu, *J. Magn. Magn. Mater.*, **214**, 176 (2000).
- [4] Y. Yermakov, A. N. Startsev, V. A. Burmistrov, *Appl. Catal.*, **11**, 1 (1984).
- [5] K. I. Tanaka, T. Okuhara, *Catal. Rev. Sci. Eng.*, **15**, 249 (1977).
- [6] T. Krogulec, A. Baranski and Z. Galus, *J. Electroanal. Chem.*, **144**, 303 (1983).
- [7] T. J. Hrynaszkiewicz, J. Kozłowski, E. Cieszyńska and T. Krogulec, *J. Electroanal. Chem.*, **367**, 213 (1994).
- [8] T. Loucka and P. Janos, *Electrochim. Acta*, **41**, 405 (1996).
- [9] J. A. Dean, *Lange's Handbook of Chemistry*, 14th ed.; McGraw-Hill, Inc.: New York (1992) Section 8.